

## Boson peak in the room-temperature molten salt tetra(*n*-butyl)ammonium croconate

Mauro C. C. Ribeiro,<sup>1,\*</sup> Luiz F. C. de Oliveira,<sup>2</sup> and N. S. Gonçalves<sup>3</sup>

<sup>1</sup>Laboratório de Espectroscopia Molecular, Instituto de Química, Universidade de São Paulo, C.P. 26077, 05513-970, São Paulo, Brazil

<sup>2</sup>Departamento de Química, Instituto de Ciências Exatas, Universidade Federal de Juiz de Fora, 36036-330, Juiz de Fora, Minas Gerais, Brazil

<sup>3</sup>Departamento de Química, Universidade Federal de Santa Catarina, C.P. 476, 88040-900, Florianópolis, Santa Catarina, Brazil

(Received 6 June 2000; published 15 February 2001)

Low-frequency ( $5\text{--}200\text{ cm}^{-1}$ ) Raman spectra of the room-temperature molten salt, tetra(*n*-butyl)ammonium croconate (TBCR),  $[(n\text{-C}_4\text{H}_9)_4\text{N}]_2\text{C}_5\text{O}_5\cdot 4\text{H}_2\text{O}$ , are reported. TBCR is a very viscous liquid with glass transition temperature  $T_g = 20^\circ\text{C}$ . According to the temperature dependence of the viscosity, TBCR has been classified as a fragile glass-forming liquid. Raman spectra of TBCR have been obtained from 360 K down to a deep supercooled state at 77 K. The boson peak is observed in the Raman spectra as long as the system is cooled below  $T_g$ . The spectra are discussed in terms of proposed theories for depolarized light scattering in glass-forming liquids.

DOI: 10.1103/PhysRevB.63.104303

PACS number(s): 78.30.Cp

### I. INTRODUCTION

Room-temperature molten salts, that is, ionic systems with low melting point, or just *ionic liquids*, have been investigated within the last 20 years due to the interest as alternative solvents for many chemical processes.<sup>1</sup> So far the most studied systems include the mixtures between aluminum (III) chloride,  $\text{AlCl}_3$ , and organic salts such as the derivatives of imidazolium or pyridinium halides, for instance, 1-ethyl-3-methyl-imidazolium chloride- $\text{AlCl}_3$  and 1-butylpyridinium chloride- $\text{AlCl}_3$  (see Fig. 1).<sup>1-3</sup> The glass transition temperature  $T_g$  in these systems can be smaller than  $-100^\circ\text{C}$ . In order to avoid the handling difficulties due to the hydrolysis of  $\text{AlCl}_3$ , efforts have been directed to prepare ionic liquids in which  $\text{AlCl}_3$  is not used, for instance, ionic liquids based on quaternary ammonium cations.<sup>4-7</sup> Much literature is now available, so that some guidance emerges for good candidates for ionic liquids. Entropic effects prompt for alkylammonium salts as good candidates, however, the viscosity of the melt would increase, and the conductivities would decrease, for long alkyl chains so that the systems would be useless for electrochemical applications. On the other hand, electronic delocalization seems to play a crucial role in lowering the melting point due to the softening of the ionic interactions, so that most of the ionic liquids include aromatic ions.

Despite the technological implications of a detailed knowing on their microscopic dynamics, the common ionic liquids mentioned above have not yet been put in the perspective of a wide phenomenology of glass-forming liquids.<sup>8</sup> Supercooled liquids are usually classified as strong or fragile according to the temperature dependence of the viscosity  $\eta$ .<sup>8,9</sup> In strong liquids ( $\text{SiO}_2$  being the archetypic one),  $\ln(\eta)\times T^{-1}$  plots follow an Arrhenius curve, and in fragile ones a much steeper behavior is observed close to  $T_g$ . This phenomenological classification now plays the role of limiting behaviors for glass-forming liquids. The scenario which emerges from inelastic neutron scattering and depolarized Raman spectra of glass-forming liquids is that relaxational contributions at very low frequency are frozen at low temperatures, and vi-

brational contributions (the so-called boson peak) dominate the spectra.<sup>8-12</sup> What is meant by high or low temperature is determined by the  $T_g$  of the material. In fragile liquids, the boson peak is observed when the system is cooled down to temperatures close or far below  $T_g$ , whereas in strong liquids it is observed already at temperatures far above  $T_g$ .<sup>13</sup> Although the relation between the intensity of the boson peak and the strength of the liquid has been observed for many different systems, further corroboration of this finding is welcome. A recent counterexample of this scenario has been reported,<sup>14</sup> namely, arsenic trioxide, whose Raman spectra show the disappearance of the boson peak in the intense relaxational contribution at temperatures close to  $T_g$ , in spite of the low fragility of this system.

The microscopic dynamics of ionic liquids has been investigated by NMR spectroscopy.<sup>15,16</sup> Raman and infrared spectra of ionic liquids have been reported only at the high (intramolecular)-frequency range, mainly in order to disclose the presence of  $\text{AlCl}_4^-$  species.<sup>17-21</sup> As intense fluorescence background seems to be commonplace in these ionic liquids, indeed it would preclude that good Raman spectra could be obtained at low frequencies. In this work, good Raman spectra at the low-frequency range have been obtained for the salt tetra(*n*-butyl)ammonium croconate (TBCR),  $[(n\text{-C}_4\text{H}_9)_4\text{N}]_2\text{C}_5\text{O}_5\cdot 4\text{H}_2\text{O}$ . The croconate anion  $\text{C}_5\text{O}_5^{2-}$  (see Fig. 1) is one member of the oxocarbon series, which are aromatic planar species with general formula  $\text{C}_n\text{O}_n^{2-}$  ( $n=3, 4, 5, 6$ ). Oxocarbon ions have been used in organic chemistry synthesis,<sup>22</sup> and their electronic and vibrational spectra have been studied in the last 20 years due to the high symmetry and the ability to form complexes with transition metals.<sup>23,24</sup> Resonance Raman spectra of oxocarbons and many of their derivatives have been studied extensively.<sup>25-27</sup> Recently, a Raman band shape analysis of the lithium salts of  $\text{C}_4\text{O}_4^{2-}$  and  $\text{C}_5\text{O}_5^{2-}$  in aqueous solution has been undertaken.<sup>28</sup> In this work, it is shown that by replacing the simple alkali cation by the large tetra(*n*-butyl)ammonium cation, a very viscous ionic liquid with a glass transition temperature  $T_g \approx 20^\circ\text{C}$  is obtained. This system is used as a

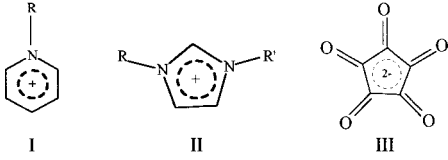


FIG. 1. The structures of the N-alkylpyridinium (I), the N,N'-dialkylimidazolium (II), and the croconate (III) ions.

prototype in order to verify whether the ionic liquids follow the above-mentioned phenomenology concerning the boson peak.

## II. THEORETICAL BACKGROUND

After Shuker and Gammon,<sup>29</sup> Raman spectra  $I(\omega)$  have been related to the vibrational density of states  $g(\omega)$  according to

$$I(\omega) = \omega^{-1} [\langle n(\omega) \rangle + 1] C(\omega) g(\omega), \quad (1)$$

where  $\langle n(\omega) \rangle$  is the Bose-Einstein population factor,  $\langle n(\omega) \rangle = [\exp(h\omega/kT) - 1]^{-1}$ , and  $C(\omega)$  is the light-vibration coupling. Depolarized Raman spectra have been reported<sup>30</sup> either in terms of the reduced Raman spectra  $I_{\text{red}}(\omega)$ ,

$$I_{\text{red}}(\omega) = I(\omega) / \{\omega [\langle n(\omega) \rangle + 1]\}, \quad (2)$$

or in terms of the susceptibility  $\chi''(\omega)$ ,

$$\chi''(\omega) = I(\omega) / [\langle n(\omega) \rangle + 1]. \quad (3)$$

The experimental Raman spectra can be fitted by a Lorentzian curve centered on the laser line, which gives the relaxational contribution, plus another function for the boson peak in the approximately 10–100-cm<sup>-1</sup> range.<sup>31,32</sup> Such an approach has been called the ‘‘superposition model,’’<sup>33</sup> as the spectra are considered as a simple superposition of the independent relaxational and vibrational contributions. Conversely, in the ‘‘coupling models,’’<sup>32–34</sup> both contributions are assumed to be strongly correlated, so that if one knows *a priori* the band shape of the vibrational contribution, one would be able to calculate the spectra in any temperature.

On the basis of the superposition model, the central line is fitted by a Lorentzian function, and the Martin and Brenig (MB) theory<sup>35</sup> is used for the calculation of the shape of the boson peak, where emphasis is put on the coupling coefficient instead on the density of states.<sup>31–33,35,37</sup> In the MB theory, the boson peak profile is due to spatial fluctuations of the wave vectors of the longitudinal (LA) and transverse (TA) acoustic phonons and dielectric properties, and is given by

$$I_{\text{boson}}(\omega) = \omega^2 [E_{\text{TA}} g_{\text{TA}}(\omega) + E_{\text{LA}} g_{\text{LA}}(\omega)], \quad (4)$$

where  $E_{\text{TA}}$  and  $E_{\text{LA}}$  are light-vibration couplings. In the original formulation, a Gaussian spatial fluctuation has been assumed, so that

$$g_{\text{TA}}(\omega) = \exp(-\omega^2/\Omega_{\text{TA}}^2), \quad (5)$$

$$g_{\text{LA}}(\omega) = (\Omega_{\text{TA}}/\Omega_{\text{LA}})^5 \exp(-\omega^2/\Omega_{\text{LA}}^2), \quad (6)$$

where the boson peak frequency is related to the corresponding sound velocities  $v$ ,  $\Omega = v/R_c$ , where  $R_c$  is the correlation length of the spatial fluctuations.

The light spectra is the Fourier transform of the fluctuation of the total polarizability,<sup>38,39</sup> given by the time correlation function  $\langle \Pi_{\alpha\beta}^{\text{total}}(\mathbf{r}, t) \Pi_{\alpha\beta}^{\text{total}}(\mathbf{r}, 0) \rangle$ , where  $\alpha$  and  $\beta$  denote any of the  $(x, y, z)$  direction, and  $\mathbf{r}$  is a shorthand notation for the coordinates of all the particles. Raman spectra have been interpreted mainly in terms of the so-called dipole-induced-dipole (DID) mechanism,  $\Pi_{\alpha\beta}^{\text{DID}}(\mathbf{r}, t)$ , plus the orientational contribution,  $\Pi_{\alpha\beta}^{\text{or}}(\Omega, t)$ , where  $\Omega$  represents the molecular orientation tensor, that is,

$$\Pi_{\alpha\beta}^{\text{total}}(\mathbf{r}, t) = \Pi_{\alpha\beta}^{\text{DID}}(\mathbf{r}, t) + \Pi_{\alpha\beta}^{\text{or}}(\Omega, t). \quad (7)$$

Both the DID and the orientational contributions imply a fully depolarized spectra, that is, the depolarization ratio  $\rho$ , should be 0.75. On the other hand, it has been observed  $\rho$  as small as 0.10 in simple (high-temperature) molten salts, such as alkali halides.<sup>40</sup> In the model of Madden *et al.*<sup>41</sup> for ionic systems, other interaction-induced mechanisms have been considered:

$$\Pi_{\alpha\beta}^{\text{total}}(\mathbf{r}, t) = \Pi_{\alpha\beta}^{\text{DID}}(\mathbf{r}, t) + \Pi_{\alpha\beta}^{\text{SR}}(\mathbf{r}, t) + \Pi_{\alpha\beta}^{\gamma}(\mathbf{r}, t) + \Pi_{\alpha\beta}^B(\Omega, t). \quad (8)$$

The  $\Pi_{\alpha\beta}^{\text{SR}}(\mathbf{r}, t)$  term is the short-range contribution which arise from first-neighbor electrostatic and overlap interactions which change the compression potential on the ionic charge density. The  $\Pi_{\alpha\beta}^{\gamma}(\mathbf{r}, t)$  and  $\Pi_{\alpha\beta}^B(\mathbf{r}, t)$  terms arise from the field and field gradient, respectively, experimented by a given ion due to the other ions. The  $\Pi_{\alpha\beta}^{\text{SR}}(\mathbf{r}, t)$  and  $\Pi_{\alpha\beta}^{\gamma}(\mathbf{r}, t)$  terms contribute to the isotropic Raman spectra, so that this model is able to explain the low  $\rho$  in molten salts.<sup>41–44</sup>

A unique feature of ionic liquids is that all of the above five mechanisms may contribute:

$$\Pi_{\alpha\beta}^{\text{total}}(\mathbf{r}, t) = \Pi_{\alpha\beta}^{\text{or}}(\Omega, t) + \Pi_{\alpha\beta}^{\text{DID}}(\mathbf{r}, t) + \Pi_{\alpha\beta}^{\text{SR}}(\mathbf{r}, t) + \Pi_{\alpha\beta}^{\gamma}(\mathbf{r}, t) + \Pi_{\alpha\beta}^B(\mathbf{r}, t). \quad (9)$$

Therefore it is not clear *a priori* what should be the value of  $\rho$  in ionic liquids: should it be low, as simple alkaly halide melts, or should it be high, as a typical organic liquid? As it will be shown in Sec. VI, in the present case of TBCR the temperature dependence of the depolarization ratio suggests that the other interaction-induced mechanisms could be also relevant.

## III. EXPERIMENT

TBCR has been obtained by the reaction in aqueous solution between  $[(n\text{-C}_4\text{H}_9)_4\text{N}]\text{I}$  (Aldrich Co. with no further purification) and the simple salt  $\text{Ag}_2\text{C}_5\text{O}_5$ , where the  $\text{C}_5\text{O}_5^{2-}$  anion has been obtained as reported previously.<sup>45</sup> By separating the  $\text{AgI}$  precipitate and slight warming of the solution in vacuum, we obtained TBCR as a very viscous liquid, which does not crystallize even after several months at rest. Rather, the system goes to a glassy state at room temperature, and becomes fluid by slight warming. The salt is soluble in water and many other solvents, such as methanol,

acetone and benzene. Elemental analysis has indicated four water molecules per  $[(n\text{-C}_4\text{H}_9)_4\text{N}]_2\text{C}_5\text{O}_5$  unity [% C = 62.8(63.8), % H = 10.8(11.5), and % N = 4.3(4.0), where the values in parentheses are the expected ones]. This is consistent with a 10.0% loss of water at 40.0 °C. The thermogravimetry of TBCR also indicates that the system is stable up to 150.0 °C.

Differential scanning calorimetry has been performed in a DSC 10 of TA Instrument. Viscosities were determined by using a rheometer CP-52 model RV-DVIII of Brookfield. Raman spectra have been recorded with a U-1000 Jobin-Yvon double monochromator spectrometer fitted with a photomultiplier tube and a photon counting electronics. The spectra were excited with the 647.1-nm line of a  $\text{Kr}^+$  laser (Coherent model 400), with approximately 150 mW of output power. Both polarized (VV) and depolarized (VH) Raman spectra in the usual 90° geometry were recorded from 5 to 300  $\text{cm}^{-1}$ , each 1  $\text{cm}^{-1}$ . The spectral resolution was 2  $\text{cm}^{-1}$ . Depolarization ratio has been measured as the quotient between depolarized and polarized spectra,  $\rho(\omega) = I_{\text{VH}}(\omega)/I_{\text{VV}}(\omega)$ . Temperature control was achieved with a Optistat<sup>DN</sup> cryostat of Oxford Instruments. The spectra at low temperature have been obtained by stepwise cooling from room temperature and then resting approximately two hours in each temperature, a period of time which included one hour equilibration period plus one hour for data acquisition. We stress that all of the spectra shown in the following have been obtained by using this cooling rate protocol, since we observed slight variation in the relative weight of the relaxational and the vibrational contributions when the system follows a different thermal history. Very recently, this finding has been noted in the strong glass former  $\text{B}_2\text{O}_3$ ,<sup>46</sup> and the fact that it is also observed in such a fragile liquid as TBCR deserves a further systematic investigation which is beyond the scope of the present paper.

#### IV. CHARACTERIZING TETRA(*n*-BUTYL)AMMONIUM CROCONATE

Before discussing the low-frequency Raman spectra of TBCR, we first put this system in the perspective of the more common ionic liquids which have been mentioned in the Introduction.<sup>1</sup> Figure 2 shows the DSC curves of TBCR, in which a single event is observed, which is assigned to the glass transition  $T_g = 20 \pm 4$  °C, where the uncertainty comes from different samples which have been subjected to distinct thermal history.  $T_g$  of TBCR should be compared with the melting point of simple tetraalkylammonium salts, for instance, tetramethyl- (420 °C), tetrapentyl- (141 °C) and tetrahexylammonium chloride (112 °C).<sup>3</sup>  $T_g$  of TBCR is smaller than the melting point of a longer alkyl chain alkylammonium chloride. Melting point or glass transition temperature in ionic liquids based on dialkylimidazolium chloride- $\text{AlCl}_3$  mixtures are strongly dependent on the composition.<sup>47</sup> In the case of the well-known 1-ethyl-3-methyl-imidazolium chloride ([EtMelm]Cl)- $\text{AlCl}_3$  mixtures, the smaller  $T_g$  (−90 °C) is achieved at a  $\text{AlCl}_3$  mole fraction equal to 0.66. (Compare with the melting point of the simple salts: [EtMelm] $\text{NO}_3$ , +38 °C; [EtMelm] $\text{NO}_2$ , +55 °C; [EtMelm] $\text{SO}_4 \cdot \text{H}_2\text{O}$ ,

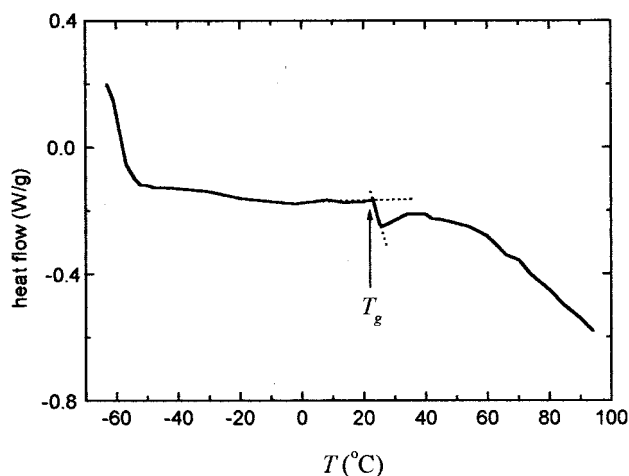


FIG. 2. DSC curves of TBCR obtained by heating the system from −60 up to +100 °C at a 10 °C/min rate.

+70 °C).<sup>4</sup> Hydrophobic ionic liquids [with no halogenoaluminates III] based on dialkylimidazolium cations have been prepared with triflate, trifluoroacetate, and other anions by Bonhôte *et al.*<sup>5</sup> The melting points or glass transition temperatures reported by these authors range from well below (−50 °C) to far above (113 °C) the  $T_g$  of TBCR. More recently, Sun *et al.*<sup>7</sup> prepared quaternary ammonium salts based on the bis(trifluoromethylsulfonyl)imide anion,  $(\text{CF}_3\text{SO}_2)_2\text{N}^-$ . The melting point of the tetrabutylammonium derivate is +96 °C. Very low  $T_g$  (<−70 °C) has been achieved in these systems either with asymmetrical cations such as  $(n\text{-C}_6\text{H}_{13})(\text{CH}_3)_3\text{N}^+$ , or with longer alkyl chains cations, for instance,  $(n\text{-C}_6\text{H}_{13})(n\text{-C}_4\text{H}_9)_3\text{N}^+$ .

A very interesting feature emerges in TBCR, that is, the low  $T_g$  with a *double* charge anion. To the authors knowledge, all of the reported ionic liquids are made of single charge species, which is not a surprise since one would expect much stronger interactions between double charge ions. Therefore the observed low  $T_g$  in TBCR points to the crucial role of electronic delocalization in the oxocarbon anion in order to soften the ionic interactions. Since double charge ions are better charge carriers than single charge ions, an ionic liquid made of double charge ions should be technologically relevant in electrochemical applications. Although the viscosity of TBCR is unfortunately too high (see below), it is promptly soluble in many solvents, and the present report should motivate further search for less viscous derivatives with lower  $T_g$ .

As the strength of a glass-forming liquid is very much related to the network characteristics in the structure of the liquid, it is expected that the ionic liquids should be classified as fragile ones. In fact, non-Arrhenius dependence of  $\eta$  with temperature have been observed in the [EtMelm]Cl- $\text{AlCl}_3$  mixtures,<sup>47</sup> and, more recently, in the ionic liquids based on N,N-dialkylimidazolium cations and several hydrofobic anions.<sup>5</sup> Interestingly, the viscosity of other well known ionic liquid, the N-alkylpyridinium chloride- $\text{AlCl}_3$  mixture, has been fitted with an Arrhenius curve.<sup>2</sup> However, one should not discard the possibility that the good fit achieved in the latter case might be due

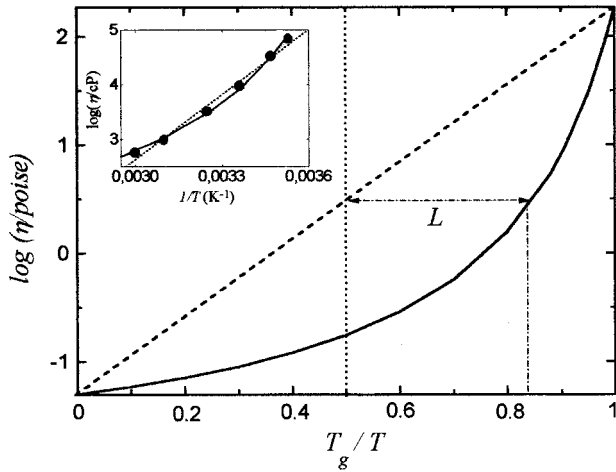


FIG. 3. Arrhenius plot of the viscosity of TBCR. The inset shows the experimental data (circles) and the VFT fit, Eq. (10), with  $B=420$  and  $T_0=238$  K (full line). For comparison, a linear (Arrhenius) dependence is shown (dotted line). In the main figure, the full line is the VFT fit and the dashed line is an exact Arrhenius dependence in the full temperature range. The latter sets the strong behavior limit. The construct to obtain  $F_{1/2}$ , which is twice the distance  $L$ , is shown as explained in the text.

to the smaller temperature range (25–75 °C) of the available experimental data than in the case of [EtMelm]Cl-AlCl<sub>3</sub> (10–90 °C). As [EtMelm]Cl-AlCl<sub>3</sub> is far the most investigated system, we will compare the viscosity of this system with TBCR.

An Arrhenius plot of  $\eta$  for TBCR is shown in the inset of Fig. 3. The experimental data do not follow an Arrhenius curve, instead they have been fitted by a Vogel-Fulcher-Tammann (VFT) equation:

$$\eta = \eta_0 \exp[B/(T - T_0)]. \quad (10)$$

Since other formulas than the VFT equation have been used to fit  $\eta(T)$  curves of ionic liquids,<sup>47</sup> we have chosen a given fragility indice in order to compare TBCR with other ionic liquids. Here we will follow closely the fragility metric  $F_{1/2}$  proposed by Angell *et al.*<sup>48</sup> The construct is shown in Fig. 3, where the full line is the fit of the experimental data with the VFT equation. Note that the temperature axis is normalized by the glass transition temperature. Equation (10) is used to extrapolate to the whole range of temperature,  $0 < T_g/T < 1$ , and a linear (dashed) curve is drawn in order to represent an exact Arrhenius dependence which would be the behavior of a strong liquid. Then a vertical (dotted) line at the midpoint of the temperature axis is drawn.  $F_{1/2}$  is defined as twice the distance  $L$ , as measured in the temperature axis, between the strong liquid behavior curve and the actual system ( $F_{1/2} = 2L$ ). In other words,  $F_{1/2}$  measures the departure of  $\eta(T)$  from an Arrhenius curve, and therefore from the strong liquid behavior.

The  $F_{1/2}$  values of TBCR and some N,N'-dialkylimidazolium chloride-AlCl<sub>3</sub> mixtures are shown in Table I. The  $F_{1/2}$  values of these mixtures have been calculated as shown in Fig. 3 by using the (not usual) equation  $\eta = AT^{1/2} \exp[k/(T - T_0)]$ , which has been fitted to the experi-

TABLE I. Glass transition temperature  $T_g$ , viscosity at 35 °C,  $\eta_{35}$ , and the fragility indice  $F_{1/2}$ , of some ionic liquids.

	$T_g$ (K)	$\eta_{35}$ (cP)	$F_{1/2}$
tetra( <i>n</i> -butyl)ammonium croconate <sup>a</sup>	293	3257.0	0.68
[EtMelm]Cl/AlCl <sub>3</sub> ( $x_{\text{AlCl}_3}=0.32$ ) <sup>b</sup>	214	1.197	0.89
[EtMelm]Cl/AlCl <sub>3</sub> ( $x_{\text{AlCl}_3}=0.42$ ) <sup>b</sup>	193	0.328	0.80
[EtMelm]Cl/AlCl <sub>3</sub> ( $x_{\text{AlCl}_3}=0.61$ ) <sup>b</sup>	179	0.118	0.66
[EtMelm]Cl/AlCl <sub>3</sub> ( $x_{\text{AlCl}_3}=0.66$ ) <sup>b</sup>	177	0.108	0.64
[ButMelm]Cl/AlCl <sub>3</sub> ( $x_{\text{AlCl}_3}=0.66$ ) <sup>b</sup>	195	0.145	0.70
[ButButlm]Cl/AlCl <sub>3</sub> ( $x_{\text{AlCl}_3}=0.66$ ) <sup>b</sup>	173	0.176	0.78
2Ca(NO <sub>3</sub> ) <sub>2</sub> ·3KNO <sub>3</sub> (CKN) <sup>c</sup>	335		0.92

<sup>a</sup>This work.

<sup>b</sup> $F_{1/2}$  has been calculated by using the experimental data given in Ref. 47.

<sup>c</sup> $F_{1/2}$  has been calculated by using the experimental data given in Ref. 49.

mental data in Ref. 47. For comparison purposes, we calculated  $F_{1/2}$  as depicted above for the archetypic fragile liquid 2Ca(NO<sub>3</sub>)<sub>2</sub>·3KNO<sub>3</sub>(CKN), by using the viscosity data of Ref. 49.

Despite much literature about N,N'-dialkylimidazolium chloride-AlCl<sub>3</sub> mixtures, to our knowledge the decreasing in  $F_{1/2}$  with increasing AlCl<sub>3</sub> content has not been stated before because these systems had not been quantified by any fragility indice. Since the strength of the liquid is related to its structure, this finding is fully in accordance with spectroscopic and theoretical evidences for the structure of these ionic liquids. On a microscopic view, the structure of fragile liquids, such as organic liquids, is dominated by packing effects, whereas in strong ones there are directional or networklike characteristics such as in SiO<sub>2</sub>. Combined usage of NMR, infrared and Raman spectroscopies, and quantum chemistry calculations<sup>17–21,50,51</sup> indicated that hydrogen bonds are formed between any of the three hydrogens of the imidazolium cation and the anions. In basic mixtures ( $0.33 < x_{\text{AlCl}_3} < 0.5$ ) the dominant anion is AlCl<sub>4</sub><sup>-</sup>, whereas in acid solution ( $x_{\text{AlCl}_3} > 0.5$ ) there are other species such as Al<sub>2</sub>Cl<sub>7</sub><sup>-</sup> and Al<sub>2</sub>Cl<sub>6</sub>. Molecular-dynamic simulations of pure MX<sub>3</sub> (high-temperature) molten salts<sup>44,52</sup> have corroborated that polarization effects on the anions play a crucial role in stabilizing these structures, which are formed by shared polyhedra. Therefore the structures which are formed at higher AlCl<sub>3</sub> content increases the strength of the liquid, giving smaller  $F_{1/2}$  values. It is clear from Table I that N,N'-dialkylimidazolium chloride-AlCl<sub>3</sub> mixtures become more fragile as longer alkyl chains are present. Interestingly, in spite of the presence of four butyl groups in TBCR, it is even stronger than [ButButlm]Cl-AlCl<sub>3</sub>, but of course it is still a fragile liquid.

## V. RAMAN SPECTRA OF TETRA(*n*-BUTYL)AMMONIUM CROCONATE

Figure 4 shows the low-frequency depolarized Raman spectra of TBCR from above the room temperature down to a deep supercooled state. The only data manipulation in Fig.

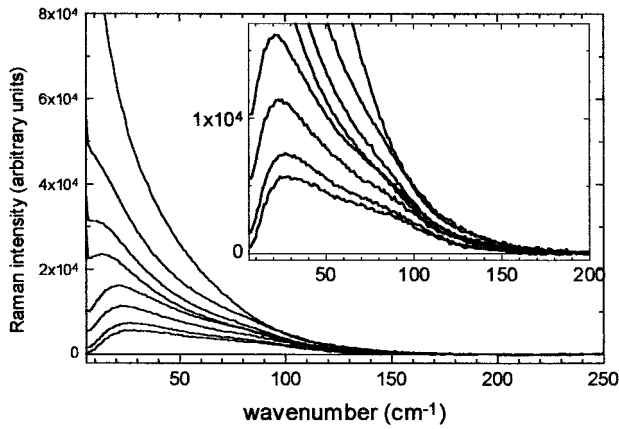


FIG. 4. Depolarized Raman spectra of TBCR. From top to bottom: 323, 293, 273, 250, 200, 150, 100, and 77 K. The inset highlights the spectra at low temperatures.

4 is a subtraction of a linear baseline which has been fitted in the 200–300-cm<sup>-1</sup> range. The figure promptly reminds us of the known features of depolarized Raman spectra of glass formers. In the case of TBCR, it is clear that the presence of another band at approximately 60 cm<sup>-1</sup>, which is the microscopic peak.<sup>31,53–56</sup> This band has been assigned to the librational motion of phenyl groups in case of aromatic systems, which is also a reasonable assignment in TBCR. It is worth mentioning that a previous Raman band shape analysis of the high-frequency (intramolecular) bands of the simple salt Li<sub>2</sub>C<sub>5</sub>O<sub>5</sub> in aqueous solution indicated the librational motion of the oxocarbon ring in approximately 80 cm<sup>-1</sup>.<sup>28</sup> At high temperatures, the Raman spectra of TBCR are given by an almost Lorentzian band whose center is located at zero frequency. At low temperatures, the boson peak at approximately 20 cm<sup>-1</sup> dominates the spectra. As discussed in Sec. II, these features have been assigned to the relaxational and the vibrational contributions, respectively, the full spectra being a simple superposition of them (the superposition model), or, conversely, a strong coupling between them occurs (the coupling model).<sup>8,14,31–34</sup> The most important observation related to Fig. 4 is that the boson peak is clearly seen in TBCR only at temperatures below  $T_g$ . At 293 K, that is, right at  $T_g$ , the boson peak is only a shoulder on the tail of the relaxational contribution. This is consistent with the fragile classification of TBCR as given by the  $\eta(T)$  curve (in contrast with strong liquids, for instance, B<sub>2</sub>O<sub>3</sub>,<sup>57,58</sup> where the boson peak is well defined even at temperatures far above  $T_g$ ).

In order to obtain the density of states  $g(\omega)$  from the Raman spectrum, the functional form of  $C(\omega)$  should be known [see Eq. (1)]. Since distinct limiting behaviors for  $C(\omega)$  have been proposed, its exact frequency dependence is other unsettled issue.<sup>43,59–63</sup> In many glass formers, a simple linear dependence,  $C(\omega) \propto \omega$ , has been proposed. In such a case, the  $\chi''(\omega)$  representation would be  $g(\omega)$  [see Eq. (3)]. In the  $\omega$ -range below the boson peak, it has been found that  $\chi''(\omega) \propto \omega^3$  for various glass formers, and, were the density of states a Debye-like one in this low- $\omega$  range,  $g(\omega) \propto \omega^2$ , the coupling coefficient would be instead  $C(\omega) \propto \omega^2$ .

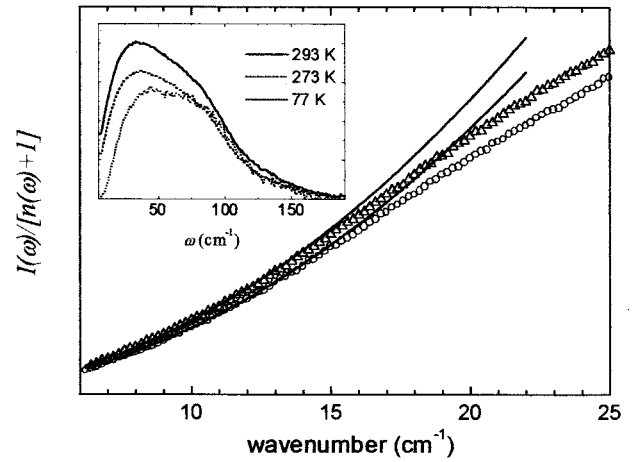


FIG. 5. The low-frequency limit of the depolarized Raman spectra in the  $\chi''(\omega)$  representation [Eq. (3)] of TBCR at 77 (circles) and 100 K (triangles). The lines indicate the quadratic dependence of  $\chi''(\omega)$  at frequencies below the boson peak. The inset shows the full  $\chi''(\omega)$  spectra at the indicated temperatures.

Neutron-scattering measurements have indicated, however, that  $g(\omega)$  exceeds the Debye limit,<sup>63</sup> although a quadratic dependence of  $g(\omega)$  has been noted in SiO<sub>2</sub> and B<sub>2</sub>O<sub>3</sub> at frequencies below  $\sim 15$  cm<sup>-1</sup>.<sup>61</sup> Recently, a comparison between Raman- and neutron-scattering spectra of amorphous polycarbonate indicated a Debye behavior at low frequencies.<sup>64</sup> Computer simulations of molten ZnCl<sub>2</sub> have also indicated that  $g(\omega)$  can follow a Debye-like behavior at low frequencies despite the fact that the normal modes have a mixed character of plane-wave and localized vibrations.<sup>65,66</sup> Figure 5 highlights the quadratic dependence of  $\chi''(\omega)$  for TBCR at low temperatures in the frequency range below the boson peak. Interestingly, a less steep quadratic dependence is observed with decreasing temperature. This finding could suggest that  $\chi''(\omega) \propto g(\omega)$ , because the Debye limit is given by<sup>67</sup>

$$g^{\text{Debye}}(\omega) = (2\pi^2)^{-1} \omega^2 (1/v_L^3 + 2/v_T^3), \quad (11)$$

and the longitudinal and transverse sound velocities,  $v_L$  and  $v_T$ , should increase with decreasing temperature. The outcome would be  $C(\omega) \propto \omega$  at such low frequencies. However, a more decisive evidence for that need comparisons between Raman- and neutron-scattering spectra. The present paper should motivate further investigations on TBCR, since it is a particularly appropriate system for neutron-scattering measurements due to the high symmetry of the oxocarbon anion.

Figure 6 shows the depolarization ratio of TBCR at temperatures close to  $T_g$ . The depolarization ratio is shown only up to 100 cm<sup>-1</sup> because the intensities of both the polarized and the depolarized spectra at high frequency are very small, and their quotient becomes very noisy. In line with observations in other glass formers,<sup>36,37,68</sup>  $\rho$  is constant in the frequency range including the relaxational and the vibrational contributions. This is the strong argument in favor of the picture of a coupling between both of the contributions.<sup>34</sup> On the other hand, in a recent investigation of the low-frequency Raman spectra of the (high-temperature) molten salt

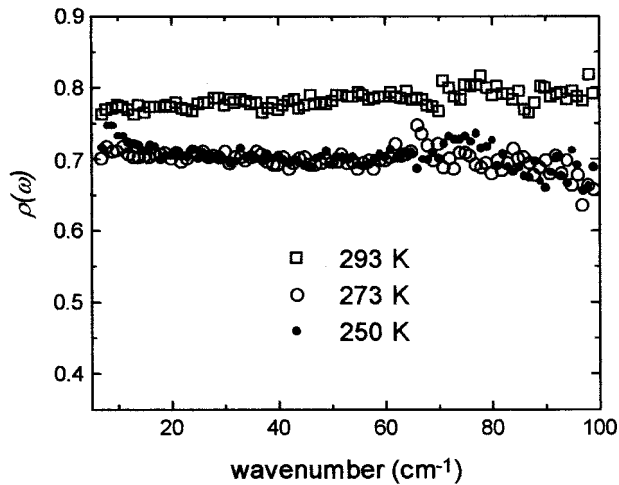


FIG. 6. Depolarization ratio,  $\rho = I_{VH}/I_{VV}$ , of TBCR at temperatures close to the glass transition.

$2\text{BiCl}_3 \cdot \text{KCl}$ , Kirillov and Yannopoulos<sup>69</sup> concluded that the superposition model should be preferred on the basis of the frequency dependence of the depolarization ratio  $\rho(\omega)$ . The same group has found frequency-dependent depolarization ratio in other glass formers.<sup>70</sup> In the case of TBCR,  $\rho$  is equal to 0.75 at  $T_g$  (and higher temperatures), whereas at temperatures below  $T_g$  a slight drop in  $\rho$  has been found. This finding should be contrasted with the temperature-independent  $\rho(\omega)$  reported recently in the case of  $\text{As}_2\text{O}_3$  and  $2\text{BiCl}_3 \cdot \text{KCl}$ .<sup>71</sup> The decrease in  $\rho$  follows the abrupt decrease in the intensity of the relaxational contribution across  $T_g$ , as noted from the fitting procedure shown in Fig. 7. The temperature dependence of  $\rho$  in TBCR suggests that the other interaction-induced mechanisms have increased weight with decreasing temperature [see Eq. (9)]. In such a case, distinct mechanisms would dominate the relaxational or the vibrational contributions, what weakens the argument in favor of the coupling models. On the basis of distinct mechanisms, however, one would expect a (slight) frequency-dependent depolarization ratio in a temperature range where both the contributions are comparable, say  $T \approx 273$  K as suggested by Fig. 7. As an alternative explanation for the not usual temperature dependence of  $\rho$  in TBCR is that an anisotropic environment develops in glassy TBCR due to the particular planar symmetry of the oxocarbon anion. This unsettled issue is a further motivation for neutron-scattering measurements or computer simulations of TBCR.

Figure 7 shows examples of the fit of the boson peak by using Eqs. (4) and (5) [since  $\Omega_{LA}$  is typically twice  $\Omega_{TA}$ , the fitting is usually done considering only the first term in Eq. (4)]. In some systems,<sup>31,36</sup> it has been found that a Gaussian shape is not able to represent a long tail at high frequencies. In such case, an exponential dependence of the spatial fluctuations has been assumed, so that  $g_{TA}(\omega)$  would be Lorentzian. Despite the presence of the microscopic peak at approximately  $60 \text{ cm}^{-1}$ , which has been fitted with an additional Gaussian function, we have found that the Lorentzian model gives a poor fit to the high-frequency tail. Other more general expressions have been also proposed to fit low-

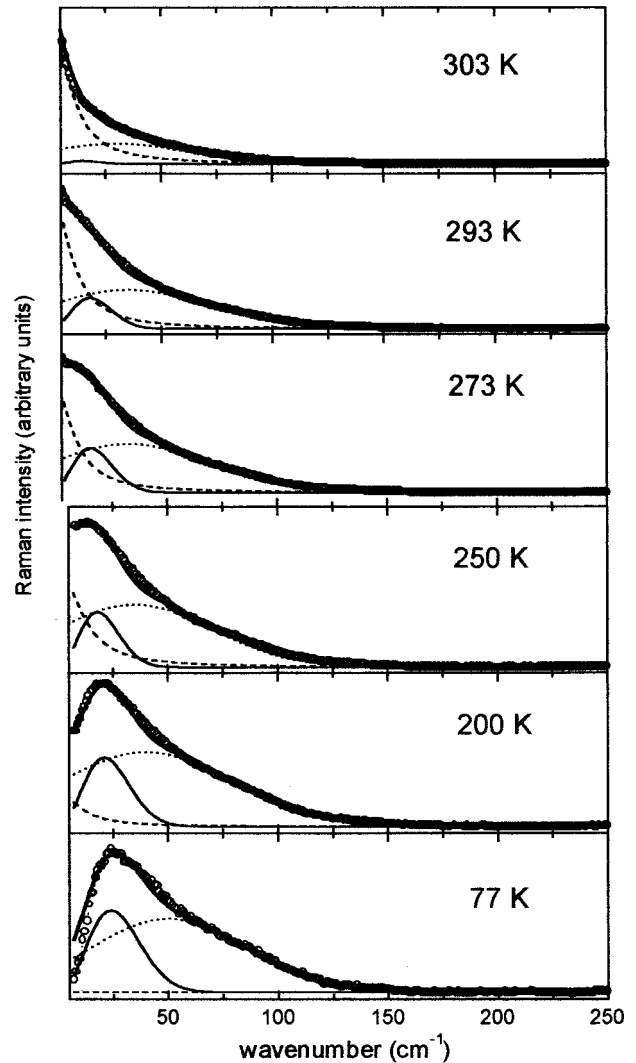


FIG. 7. Best fit of the reduced depolarized Raman spectra [Eq. (2)] of TBCR by using Eqs. (4) and (5). At each temperature, we show the experimental data (circles), the best fit (bold line superimposed on the experimental data), the relaxational contribution (dashed line), the microscopic peak (dotted line), and the boson peak (full line).

frequency Raman spectra,<sup>31,32,36,69</sup> which we did not attempt to use due to the increasing number of adjustable parameters. Very recently,<sup>69</sup> these fitting procedures have been applied to both the polarized and the depolarized Raman spectra, so that the depolarization ratio of each of the contributions have been obtained. In the present case of TBCR, the same set of parameters, except by a scale factor, gives reasonable fitting of both the polarized and the depolarized Raman spectra, so that the depolarization ratio is the same for the relaxational and the vibrational contributions.

The frequency of the microscopic peak decreases smoothly with temperature (see Fig. 8), but its width ( $45 \text{ cm}^{-1}$ ) is almost unchanged in all temperatures. In line with previous findings, the width of the central Lorentzian line ( $20.0 \text{ cm}^{-1}$ ) is almost unchanged at different temperatures, whereas the boson peak frequency decreases only slightly with cooling (Fig. 8). Therefore the only parameter which

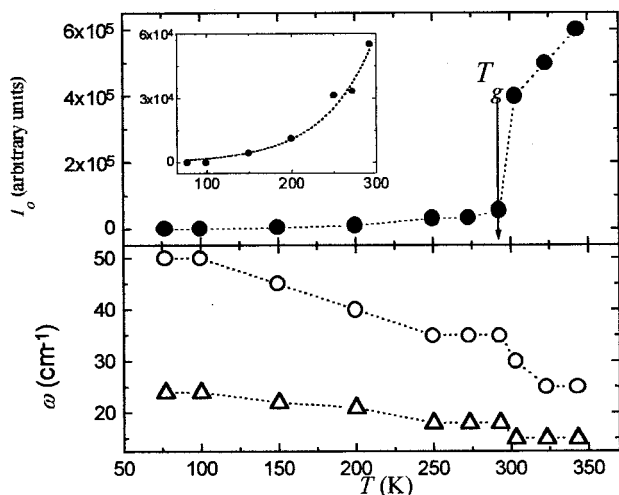


FIG. 8. Temperature dependence of the best-fit parameters. Top panel: the intensity of the central Lorentzian contribution (the dotted line is a guide to the eye). The inset highlights the temperature dependence up to the glass transition temperature (the dotted line is an exponential fit). Bottom panel: frequency of the microscopic peak (circles) and the boson peak (triangles). The dotted line is a guide to the eye.

suffers a substantial temperature dependence is the intensity of the central line  $I_0$ . As shown in Fig. 8,  $I_0$  has a smooth increase in a temperature range up to  $T_g$ , above which a sharp increase is observed. This discontinuity in  $I_0$  has been also observed in other glass-forming liquids,<sup>33,36</sup> and seems to be a rather general signature of the prompt domain of the relaxational contributions at temperatures right above  $T_g$ .

## VI. CONCLUDING REMARKS

We have shown that TBCR is a fragile glass-forming liquid. A fragility indice has been used in order to compare this

new system with other well-known low-temperature molten salts. In comparison with the more usual ionic liquids, TBCR is a much more viscous liquid, what is an obstacle for its application as an alternative solvent in organic synthesis. However, its prompt solubility in organic solvents should be stressed, since ionic liquids have been used either in a pure form or in solution, typically in aromatic solvents. TBCR has been used here as a representative example of ionic liquids in order to investigate whether the competition of relaxational versus vibrational contributions in Raman spectra of glass-forming liquids is also observed in these systems. We have found that the boson peak is observed in the low-frequency range of the Raman spectra as long as the system is cooled below its glass transition temperature ( $T_g \approx 20^\circ\text{C}$ ). This finding follows previously proposed correlations between the intensity of the boson peak and the strength of the liquid, since the boson peak has been observed in fragile liquids only in a deep supercooled state. The superposition model has been used in order to fit the experimental spectra from the liquid down to glassy TBCR. It has been found that the depolarization ratio is constant in the whole low-frequency range, however, its value decreases with decreasing temperature. In addition to the DID and the reorientational contributions, other interaction-induced mechanisms can contribute in the fluctuation of the polarizability in ionic liquids. The temperature dependence of the depolarization ratio could be interpreted by the dominance of different mechanisms as the relaxational contribution decrease or by an orientational order which develops in TBCR at low temperatures.

## ACKNOWLEDGMENTS

The authors acknowledge the help of Professor M. R. Alcantara and E. G. Fernandes, Jr. for the viscosity measurements, Professor Y. Kawano and L. G. Lage for the DSC measurements, and Professor O. Sala for the cryostat setup. The financial support of CNPq, FAPEMIG, and FAPESP is also acknowledged.

\*Corresponding author. Email address: mccribei@quim.iq.usp.br

<sup>1</sup>See the recent reviews: K. R. Seddon, *J. Chem. Technol. Biotechnol.* **68**, 351 (1997); Y. Zhao and T. J. V. Noot, *Electrochim. Acta* **42**, 3 (1997); T. Welton, *Chem. Rev.* **99**, 2071 (1999).

<sup>2</sup>R. A. Carpio, L. A. King, R. E. Lindstrom, J. C. Nardi, and C. L. Hussey, *J. Electrochem. Soc.* **126**, 1644 (1979).

<sup>3</sup>S. D. Jones and G. E. Blomgren, *J. Electrochem. Soc.* **136**, 424 (1989).

<sup>4</sup>J. S. Wilkes and M. J. Zaworotko, *J. Chem. Soc. Chem. Commun.* **13**, 965 (1992).

<sup>5</sup>P. Bonhôte, A.-P. Dias, N. Papageorgiou, K. Kalyanasundaram, and M. Grätzel, *Inorg. Chem.* **35**, 1168 (1996).

<sup>6</sup>D. R. MacFarlane, P. Meakin, J. Sun, N. Amini, and M. Forsyth, *J. Phys. Chem.* **103**, 4164 (1999).

<sup>7</sup>J. Sun, M. Forsyth, and D. R. MacFarlane, *J. Phys. Chem. B* **102**, 8858 (1998).

<sup>8</sup>See the special issues: *Philos. Mag. B* **77**, No. 2 (1998); *J. Non-Cryst. Solids* **235-237** (1998); *J. Phys.: Condens. Matter* **11**, No. 10A (1999); *J. Phys. Chem.* **103**, No. 20 (1999); *J. Phys.: Condens. Matter* **12**, No. 8A (2000).

<sup>9</sup>C. A. Angell, *Science* **267**, 1924 (1995).

<sup>10</sup>D. Quitmann and M. Soltwisch, *Philos. Mag. B* **77**, 287 (1998).

<sup>11</sup>F. J. Bermejo, A. Criado, and J. L. Martinez, *Phys. Lett. A* **195**, 236 (1994).

<sup>12</sup>P. Benassi, M. Krisch, C. Masciovecchio, V. Mazzacurati, G. Monaco, G. Ruocco, F. Sette, and R. Verbeni, *Phys. Rev. Lett.* **77**, 3835 (1996).

<sup>13</sup>A. K. Hassan, L. Börjesson, and L. M. Torrel, *J. Non-Cryst. Solids* **172-174**, 154 (1994).

<sup>14</sup>S. N. Yannopoulos, G. N. Papatheodorou, and G. Fytas, *J. Chem. Phys.* **107**, 1341 (1997).

<sup>15</sup>C. E. Keller and W. R. Carper, *Inorg. Chim. Acta* **238**, 115 (1995).

<sup>16</sup>W. R. Carper, G. J. Mains, B. J. Piersma, S. L. Mansfield, and C. K. Larive, *J. Phys. Chem.* **100**, 4724 (1996).

<sup>17</sup>R. J. Gale, B. Gilbert, and R. A. Osteryoung, *Inorg. Chem.* **17**, 2728 (1978).

<sup>18</sup>S. Tait and R. A. Osteryoung, *Inorg. Chem.* **23**, 4352 (1984).

<sup>19</sup>K. M. Dieter, C. J. Dymek, Jr., N. E. Heimer, J. W. Rovang, and J. S. Wilkes, *J. Am. Chem. Soc.* **110**, 2722 (1988).

- <sup>20</sup>Y. S. Fung and S. M. Chau, *Inorg. Chem.* **34**, 2371 (1995).
- <sup>21</sup>S. Takashi, L. A. Curtis, D. Gosztola, N. Koura, and M.-L. Saboungi, *Inorg. Chem.* **34**, 2990 (1995).
- <sup>22</sup>P. V. Schleyer, K. Najafian, B. Kiran, and H. J. Jiao, *J. Org. Chem.* **65**, 426 (2000).
- <sup>23</sup>W. C. Herndon, *J. Mol. Struct.: THEOCHEM* **103**, 219 (1983).
- <sup>24</sup>H. Torii and M. Tasumi, *J. Mol. Struct.: THEOCHEM* **334**, 15 (1995).
- <sup>25</sup>P. S. Santos, J. H. Amaral, and L. F. C. de Oliveira, *J. Mol. Struct.* **243**, 223 (1991).
- <sup>26</sup>L. F. C. de Oliveira and P. S. Santos, *J. Mol. Struct.* **269**, 85 (1992).
- <sup>27</sup>L. K. Noda, N. S. Gonçalves, P. S. Santos, and O. Sala, *J. Braz. Chem. Soc.* **7**, 385 (1996).
- <sup>28</sup>M. C. C. Ribeiro, L. F. C. de Oliveira, and P. S. Santos, *Chem. Phys.* **217**, 71 (1997).
- <sup>29</sup>R. Shuker and R. W. Gammon, *Phys. Rev. Lett.* **25**, 222 (1970).
- <sup>30</sup>A. P. Sokolov, A. Kisliuk, D. Quitmann, A. Kudlik, and E. Rössler, *J. Non-Cryst. Solids* **172-174**, 138 (1994).
- <sup>31</sup>S. A. Kirillov, T. S. Perova, O. F. Nielsen, E. Praestgaard, U. Rasmussen, T. M. Kolomiyets, G. A. Voyiatzis, and S. H. Anastasiadis, *J. Mol. Struct.* **479**, 271 (1999).
- <sup>32</sup>S. A. Kirillov, *J. Mol. Struct.* **479**, 279 (1999).
- <sup>33</sup>F. Terki, C. Levelut, J. L. Prat, M. Boissier, and J. Pelous, *J. Phys.: Condens. Matter* **9**, 3955 (1997).
- <sup>34</sup>V. Z. Goshiyaev, V. K. Malinowsky, V. N. Novikov, and A. P. Sokolov, *Philos. Mag.* **63**, 777 (1991).
- <sup>35</sup>A. J. Martin and W. Brenig, *Phys. Status Solidi B* **64**, 163 (1974).
- <sup>36</sup>M. Krüger, M. Soltwisch, I. Petscherizin, and D. Quitmann, *J. Chem. Phys.* **96**, 7352 (1992).
- <sup>37</sup>J. Lorösch, M. Couzi, J. Pelous, R. Vacher, and A. Levasseur, *J. Non-Cryst. Solids* **69**, 1 (1984).
- <sup>38</sup>H. Z. Cummins, G. Li, W. Du, R. M. Pick, and C. Dreyfus, *Phys. Rev. E* **53**, 896 (1996).
- <sup>39</sup>A. Patkowski, W. Steffen, H. Nilgens, E. W. Fischer, and R. Pecora, *J. Chem. Phys.* **106**, 8401 (1997).
- <sup>40</sup>R. K. McGreevy, *Solid State Phys.* **40**, 247 (1987).
- <sup>41</sup>P. A. Madden, K. O'Sullivan, J. A. Board, and P. W. Fowler, *J. Chem. Phys.* **94**, 918 (1991).
- <sup>42</sup>P. A. Madden and K. F. O'Sullivan, *J. Chem. Phys.* **95**, 1980 (1991).
- <sup>43</sup>M. C. C. Ribeiro, M. Wilson, and P. A. Madden, *J. Chem. Phys.* **110**, 4803 (1999).
- <sup>44</sup>M. J. Castiglione, M. C. C. Ribeiro, M. Wilson, and P. A. Madden, *Z. Naturforsch., A: Phys. Sci.* **54**, 605 (1999).
- <sup>45</sup>N. S. Gonçalves, P. S. Santos, and I. Vencato, *Acta Crystallogr., Sect. C: Cryst. Struct. Commun.* **52**, 622 (1996).
- <sup>46</sup>N. V. Surovtsev, J. Wiedersich, A. E. Batalov, V. N. Novikov, M. A. Ramos, and E. Rössler, *J. Chem. Phys.* **113**, 5891 (2000).
- <sup>47</sup>A. A. Fannin, Jr., D. A. Floreani, L. A. King, J. S. Landers, B. J. Piersma, D. J. Stech, R. L. Vaughn, J. S. Wilkes, and J. L. Williams, *J. Phys. Chem.* **88**, 2614 (1984).
- <sup>48</sup>C. A. Angell, B. E. Richards, and V. Velikov, *J. Phys.: Condens. Matter* **11**, A75 (1999).
- <sup>49</sup>E. Veliyulin, E. Shasha, A. Voronel, V. S. Machavariani, S. Seifer, Y. Rosenberg, and M. G. Shumsky, *J. Phys.: Condens. Matter* **11**, 8773 (1999).
- <sup>50</sup>W. R. Carper, J. L. Pflug, A. M. Elias, and J. S. Wilkes, *J. Phys. Chem.* **96**, 3828 (1992).
- <sup>51</sup>A. G. Avent, P. A. Chaloner, M. P. Day, K. R. Seddon, and T. Welton, *J. Chem. Soc. Dalton Trans.* **23**, 3405 (1994).
- <sup>52</sup>F. Hutchinson, A. J. Rowley, M. K. Walters, M. Wilson, P. A. Madden, J. C. Wasse, and P. S. Salmon, *J. Chem. Phys.* **111**, 2028 (1999).
- <sup>53</sup>A. Patkowski, W. Steffen, G. Meier, and E. W. Fischer, *J. Non-Cryst. Solids* **172-174**, 52 (1994).
- <sup>54</sup>C. Alba-Simionesco and M. Krauzman, *J. Chem. Phys.* **102**, 6574 (1995).
- <sup>55</sup>C. Alba-Simionesco, V. Krakoviack, M. Krauzman, P. Migliardo, and F. Romain, *J. Raman Spectrosc.* **27**, 715 (1996).
- <sup>56</sup>A. Hédoux, Y. Guinet, and M. Descamps, *Phys. Rev. B* **58**, 31 (1998).
- <sup>57</sup>A. P. Sokolov, E. Rössler, A. Kisliuk, and D. Quitmann, *Phys. Rev. Lett.* **71**, 2062 (1993).
- <sup>58</sup>A. Brodin, L. Börjesson, D. Engberg, L. M. Torell, and A. P. Sokolov, *Phys. Rev. B* **53**, 11 511 (1996).
- <sup>59</sup>F. L. Galeener, A. J. Leadbetter, and M. W. Stringfellow, *Phys. Rev. B* **27**, 1052 (1983).
- <sup>60</sup>A. P. Sokolov, A. Kisliuk, M. Soltwisch, and D. Quitmann, *Phys. Rev. Lett.* **69**, 1540 (1992).
- <sup>61</sup>A. P. Sokolov, A. Kisliuk, D. Quitmann, and E. Duval, *Phys. Rev. B* **48**, 7692 (1993).
- <sup>62</sup>J. Wuttke, J. Hernandez, G. Li, G. Coddens, H. Z. Cummins, F. Fujara, W. Petry, and H. Sillescu, *Phys. Rev. Lett.* **72**, 3052 (1994).
- <sup>63</sup>A. P. Sokolov, U. Buchenau, W. Steffen, B. Frick, and A. Wischnewski, *Phys. Rev. B* **52**, R9815 (1995).
- <sup>64</sup>L. Saviot, E. Duval, N. Surovtsev, J. F. Jal, and A. J. Dianoux, *Phys. Rev. B* **60**, 18 (1999).
- <sup>65</sup>M. C. C. Ribeiro, M. Wilson, and P. A. Madden, *J. Chem. Phys.* **108**, 9027 (1998).
- <sup>66</sup>M. C. C. Ribeiro, M. Wilson, and P. A. Madden, *J. Chem. Phys.* **109**, 9859 (1998).
- <sup>67</sup>J. S. Blakemore, *Solid State Physics* (Cambridge University Press, Cambridge, 1985).
- <sup>68</sup>S. Kojima and V. N. Novikov, *Phys. Rev. B* **54**, 222 (1996).
- <sup>69</sup>S. A. Kirillov and S. N. Yannopoulos, *Phys. Rev. B* **61**, 11 391 (2000).
- <sup>70</sup>S. N. Yannopoulos and G. N. Papatheodorou, *Phys. Rev. B* **62**, 3728 (2000).
- <sup>71</sup>S. N. Yannopoulos, *J. Chem. Phys.* **113**, 5868 (2000).